

COMPUTATIONAL FLUID DYNAMICS OPTIMISATION OF A PELLETT BURNER

by

Lars B. WESTERLUND*, **Roger L. HERMANSSON**, and
Michel J. CERVANTES

Divisions of Energy Engineering, Fluid Mechanics, Lulea University of Technology, Lulea, Sweden

Original scientific paper
DOI: 10.2298/TSCI110609135W

Increased capacity of computers has made the computational fluid dynamics technology attractive for the design of different apparatuses. Optimisation of a pellet burner using the computational fluid dynamics was investigated in this paper. To make the design tool work fast, an approach with only mixing of gases was simulated. Other important phenomena such as chemical reactions were omitted in order to speed up the design process. The original design of the burner gave unsatisfactory performance. The optimised design achieved from simulation was validated and the results show a significant improvement. The power output increased and the emission of unburned species decreased but could be further reduced. The contact time between combustion gases and secondary air was probably too short. An increased contact time in high temperature conditions would possibly improve the design further.

Key words: *computational fluid dynamics, combustion, design, optimisation, pellet burner*

Introduction

Pellets made from biomass have become a very popular fuel to use in stoves and domestic boilers. Pellet burners are often used to retrofit boilers designed for other fuels like oil or wood logs. In Sweden most pellets are made from stem wood and the demand for this type of pellet is now exceeding the supply. New raw materials have to be used for the pellet production, for example other parts of the tree, like branches, crowns and stubs. Reed canary grass is another possible raw material. A common property of these materials is that they contain more ashes and often ashes with a tendency to sinter, which makes them less suitable for the present burners in pellet stoves and boilers [1-5].

New burners need to be developed to deal with these demanding fuels. This project aims to investigate whether the computational fluid dynamics (CFD) can be used to improve and speed up the design process. To obtain good combustion there are three conditions that are essential: temperature, turbulence and time have to fulfil certain criteria:

- the temperature has to be high enough since the reaction rate is extremely dependent on temperature,
- the mixing of the reacting species has to be as good and as fast as possible; a high degree of turbulence is necessary, and

* Corresponding author; e-mail: lars.westerlund@ltu.se

- the residence time of the mixed species in a hot environment has to be long enough.

Numerical development of a burner/furnace usually takes combustion chemistry into account. This involves many additional equations to solve, requiring large computational efforts [6-9]. Such an approach may not be appropriate for an optimisation purpose, where many simulations are needed. In the present work, a new approach is investigated. The method involves the mixing of only one species, air, where the Navier-Stokes equations are solved together with the energy equation. The main reason for such simplification is that combustion is enhanced by good mixing and residence time. Optimising such a characteristic in the burner may result in an effective burner. Comparing the CPU time for a normal run with this approach took 10-15 hours. With combustion chemistry included as in [6] (different geometry but only 20% more cells), the CPU time was 2-3 weeks.

In order to validate the model, a pellet burner aimed for demanding fuels was made available for this project [10]. The burner was tested for different fuels. It worked without interruption for most fuels but with too high emissions of harmful gases. In the present work, the optimisation of this burner using a simplified model is presented. The main goal was to improve the mixing of combustible gases from the fuel bed with secondary air to obtain an optimal mixing and economic use of air for the combustion. The best design obtained in the simulations was then implemented in the burner and tested against the original design.

Test facilities

The existing burner is presented in fig. 1. Picture (a) shows the burner fired with wood pellets. Picture (b) shows burner details and surfaces used in simulations for results analysis.

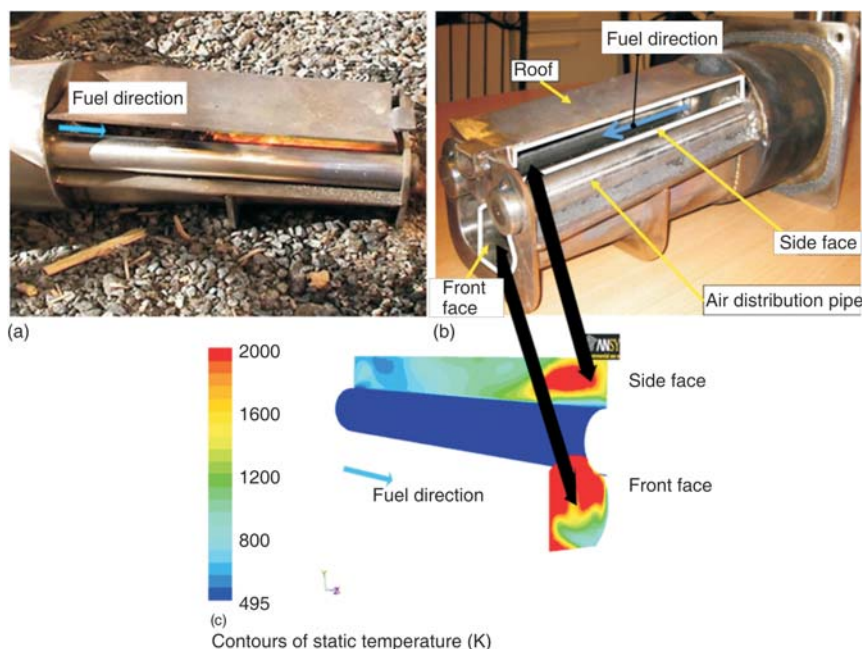


Figure 1. Burner situated outdoors on the ground (a), side view of the burner with details and surfaces used in simulations (b-c)

Looking into the burner through the front face (picture b) gives a view of interesting surfaces exemplified in picture (c).

In fig. 1(a) the pellets enter the burner from the left end with the help of a screw conveyor. They move along the bottom of the burner while burning and leave at the right end as ashes. Air is fed through two tubes above the fuel bed with holes drilled to provide air down to the bed as primary air and slightly above a horizontal line as secondary air under the roof. It is easy to change the air distribution pipes and thereby the air distribution.

The rate of fuel feeding the burner is determined by the desired power output and so is the flow of air to the burner. In the original design, the intention was that the combustion gases should leave the burner between the air tubes and the roof and be penetrated by secondary air. However, parts of the gases leave through the burner outlet on the right, fig. 1(a), and thus do not meet the secondary air.

The rate by which the fuel moves on the bed is changed as a function of the power output. Therefore, the location along the burner of the most intense combustion is also a function of the power output. Air supply should therefore be unevenly distributed along the burner. Its distribution is optimised for one power output.

Measurements on the stack gases show weaknesses of the original design. Stack gases contain too high levels of CO, which indicates poor combustion, probably due to a poor air distribution. Furthermore, there are high values of excess air and the desired power output of 20 kW is not obtained. A fact that is illustrated in fig. 1(a); the combustion on the bed takes place only on about 2/3 of the burner length.

In the simulations (see fig. 1(b-c)), surfaces are defined by the roof and the surfaces "side face" and "front face". Through these two faces the major part of the gas leaves the burner. The size inside the burner is $L \times W \times H$: 238 × 86 × 86-110 mm.

Numerical simulations

The CFD program ANSYS 12.1 was used throughout this work. The preprocessor GAMBIT was used to construct the geometry and mesh used in the solver Fluent. In order to improve the air supply, *i. e.* to obtain a better mixing of gases and a better use of the air, the method was to redistribute the holes for air supply and to change their diameter. Better mixing would be indicated by an even temperature on surfaces where gas was leaving the burner. If secondary air was introduced close to the "side face" (see fig. 1(b-c)), the control was performed on faces outside the burner.

Numerical domain

The work started with simulations of the distribution pipe for air feeding. The pipe is 238 mm long with an inner diameter of 26.64 mm and a wall thickness of 3.38 mm. The distribution pipe was the main geometrical variable in the design optimisation and was initially investigated in details before simplification. Figure 2 represents the initial design, where two types of air inlet holes are visible: primary and secondary. For the primary air inlet, the first row of holes points vertically downwards, the second row 35° and the third row 50° from the vertical line. Rows one and two

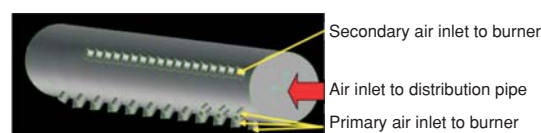


Figure 2. Air distribution pipe, inside face and pipe thickness included

contained 11 holes each with a diameter of 3.5 mm separated by 20 mm. The third row has three holes with a diameter of 3 mm separated by 20 mm. The secondary air row points 20 degrees above the horizontal line and consists of 18 holes with a diameter of 4 mm separated by 10 mm. An unstructured mesh with a total of 921340 cells was used for the simulations. Back flow through certain holes made it necessary to include a volume outside the holes.

Simulation of the entire geometry was made with a simplified model of the distribution pipe. Only the outside surface of the distribution pipe was considered and divided into smaller faces along the total length. These faces were meshed as a structured grid with a cell dimension of about 1×1 mm. User-defined functions (UDF) were used to handle the desired faces as inlet boundary for primary and secondary air supply. For cell face centres the velocity was set at zero value (wall) or desired velocity (air inlet), a process that is fast and easy to implement. The present modelling uses square holes with a cross-sectional area similar to the circular real drilled holes.

The computational domain for the entire geometry is represented in fig. 3. Half of the domain is considered for the simulations due to symmetry. The dimensions of the computational domain are $L \times W \times H = 480 \times 240 \times 400$ mm. The fuel bed is modelled as a porous medium with heat and mass release. Its volume decreases down the burner to model pellets burning. An unstructured mesh with a total number of 794822 cells was used. The reason for the low number of cells is the large number of air inlet configurations that need to be investigated. Higher mesh density was used in the burner where large gradients occur.

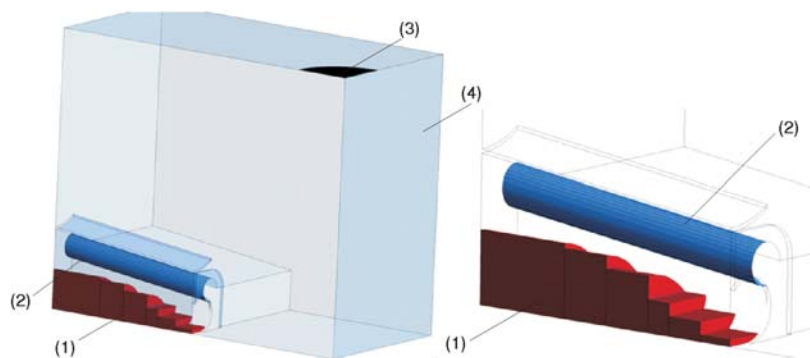


Figure 3. Computational domain used for the simulation: pellets bed (1), air inlet (2), outlet (3) and walls (4). Total domain, furnace (left), burner (right)

Numerical model

Steady state simulations were performed using the standard $k-\varepsilon$ turbulence model together with wall function and convective heat transfer. The pressure velocity coupling was solved using the SIMPLE scheme, while the Green-Gauss node-based method was used to compute the different gradients. First order upwind was used otherwise.

Simulations were performed for a maximal power output of 20 kW. The corresponding amounts of fuel, air and stack gases were determined theoretically with the software fluegas [11]. The stack gas temperature was set at $T = 450$ K. The total supply of air (54 kg/h) was set to give 10% O_2 in stack gases. The difference between the amount of stack gases and the total air supply was set to be released as air from the pellet bed. Since the span of temperature is large in the burner, varying air properties were used. The specific heat capacity for air was calculated ac-

according to a polynomial fit from tabulated values [12]. The air density was calculated from the temperature using the ideal gas law. Buoyancy was included in the simulations. The heat transfer rate from the gases inside the burner to the air distribution pipe was estimated from early simulations to 1 kW. Such heat transfer will heat the air distribution pipe to about $T = 430$ °K. This temperature was used as surface temperature for the distribution pipe as well as feed air. For the outer walls of the furnace a constant temperature of 350 K was set, all other surfaces were given adiabatic conditions.

The bed was simulated as a porous medium divided into six different parts, see fig. 3 (right). From ocular investigation of early experiments, different parts of the fuel bed were given values of mass and heat sources according to tab. 1. The fuel bed was given numbers (1-6) from burner inlet to outlet. The pellets start to burn some distance from the inlet, and therefore section 1 was given 10% of the total value of mass released from the fuel bed.

Table 1. Values used for different parts of the fuel bed

Fuel bed part	1	2	3	4	5	6
Mass source, [kgs ⁻¹]	$0.625 \cdot 10^{-4}$	$1.875 \cdot 10^{-4}$	$1.875 \cdot 10^{-4}$	$1.25 \cdot 10^{-4}$	$0.5 \cdot 10^{-4}$	$0.125 \cdot 10^{-4}$
Porosity, [%]	50	50	50	50	50	50
Max. temperature, [K]	2000	2000	2000	2000	2000	2000
Heat source, [kW]	1	3	3	2	0.8	0.2

The relative velocity resistance formulation and inertial resistance were used to simulate the fuel bed. Viscous resistance was calculated at $1.875 \cdot 10^7$ per m² and inertial resistance at 3500 per m in all three directions, values calculated for particles with a characteristic diameter of 4 mm [13]. A heat source in the bed was introduced and maximum temperature in the bed limited to 2000 K. This gave partial penetration of air into the fuel bed and total heat and mass transfer rates according to predetermined values.

The scaled mass residual decreased to $2 \cdot 10^{-4}$ before the calculations were stopped. A normal runtime for a simulation was only 3-6 hours on a computer using three processors.

The burner mounted inside the furnace includes distribution pipes and fuel bed, see fig. 3 (left).

Results

Air distribution pipe

The initially designed air distribution pipe was investigated numerically with an inlet velocity of 15.4 m/s. Figure 4 shows the air mass flow through each hole. The flow through the holes increases along the distribution pipe. The area relation between the distribution pipe and the total area of the holes is not appropriate for an even distribution. The difference between the mass flow through the primary and second-

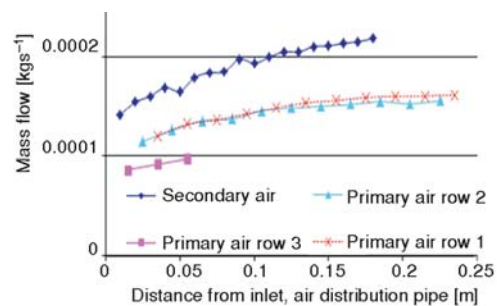


Figure 4. Air mass flow through each hole in the air distribution pipe

ary holes at the beginning and the end of the pipe is for each row about 30% and 48% respectively.

Backflow through a part of the first holes was observed. For the primary rows, small amounts of backflow exist for the first four holes. For the secondary air row, backflow occurs in the first 8 holes due to a larger diameter, fig. 5. The increased hole diameter also resulted in larger differences in velocities.

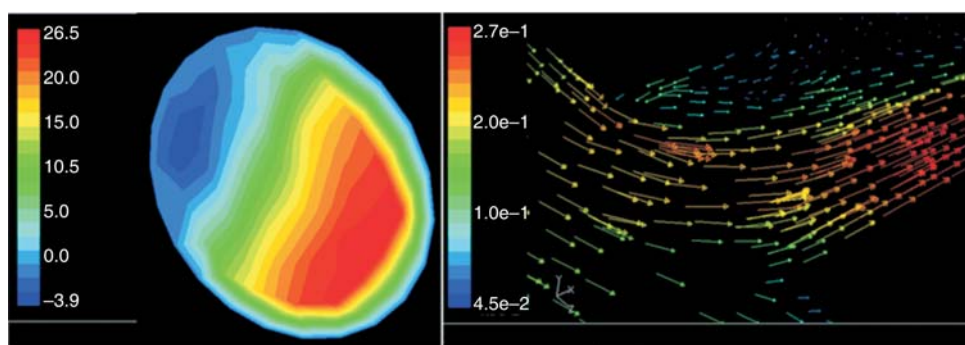


Figure 5. The distribution of velocity magnitude (left) for the outlet surface of the first hole in the secondary air row and a vector plot of the flow path (right)

Backflow through an air hole is negative for the burner performance. Combustion gases are sucked in and dirt in this gas may clog the hole. Burning of difficult fuels had in practice resulted in malfunction of the burner and the holes had to be drilled up due to clogging. This indicates that the simulation shows a reasonable flow path. A larger diameter of the air distribution pipe may increase the pressure in the distribution pipe; a more even air distribution may thus be obtained and the tendency towards backflow be decreased.

Initial burner design

Experimental investigation

A number of experiments with the original burner design were performed. Two different fuels were used in the tests: wood pellets and pellets made from reed canary grass. The combustion was not satisfactory, which can be seen in tab. 2.

Table 2. Load and outlet gas concentration with the initial burner design

Fuel	Load, [%]	O ₂ , [%]	CO, [ppm]	NO _x , [ppm]
Wood	100	15.3	1288	23
Wood	60	17.5	1037	10
Wood	30	8.5	590	27
Reed canary grass	100	15.6	812	142
Reed canary grass	60	13.4	608	123
Reed canary grass	30	14	420	85

The desired power output of 20 kW at full load could not be obtained. The maximum power output was about 15 kW. The values for excess air and CO were too high. The air is probably not distributed in the best way in the burner. Much of the combustion takes place in the latter part of the burner where there is no supply of secondary air. In this part there is a deficit of air while there is too much secondary air in other positions. Table 2 also shows high emissions of NO_x from reed canary grass due to the higher content of nitrogen in this fuel. Figure 6 shows that a considerable amount of combustion gases leaves the burner in the forward direction where secondary air is absent.



Figure 6. Combustion of wood pellets in the burner of original design

Simulation

Simulation of the burner with uniform air distribution along the pipe and with original hole location gave the following results (fig. 7) for temperature and velocity distribution for the “side” and “front” faces.

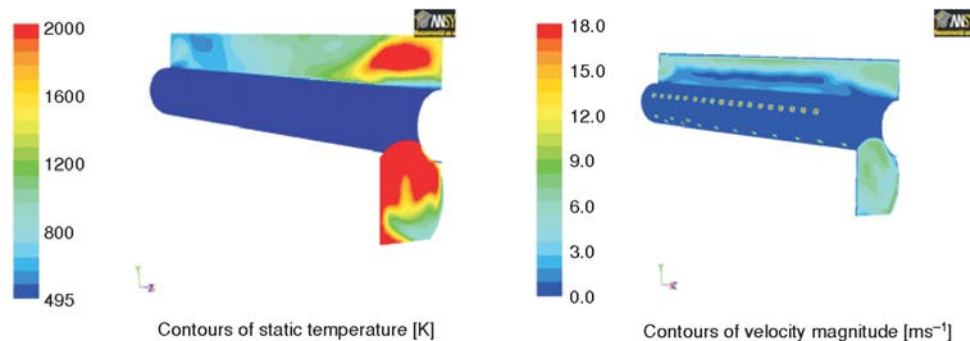


Figure 7. Contour plot of temperature (left) and velocity (right) distribution on side and front faces, original design

The temperature at the end of the burner is too high, since no secondary air is supplied at the end of the air distribution pipe (see fig. 2) and no mixing occurs. The mass flow through these faces and flow of stack gases from the furnace are presented in tab. 3. About 21% of the total mass flow passes through the front face. The total mass flow rate also includes a small portion of gas leaving the burner through an opening between the bent roof and the front wall of the burner. This gas flow has a very high temperature. Through the last part of the fuel bed some gas leaves the burner (0.3%) due to the porous medium settings. In fig. 7, the right part shows the velocity distribution with highest values (6.5 m/s) close to the roof on the side face and more evenly high velocities on the front face. The high temperature areas (red part in fig. 7, left) may be interpreted as CO gases leaving the burner without any oxygen present.

Both experiments and simulation show disadvantages in the original design. Poor mixing (high temperature levels) occurs through the front face and for the side face close to this zone. These areas contribute to the high CO levels in measurement of stack gases.

Table 3. Average values for mass flow rates

Surface	Mass flow rate, [kgs ⁻¹]	Distribution of mass flow rates, [%]
Front	0.00159	21
Side	0.00580	77
Outlet	0.00752	100

Burner optimisation and validation

Burner optimisation

To distribute the secondary air more evenly, the hole size was changed to 3.4 mm in diameter, the number of holes was increased to 24 with 9 mm space distance between the holes to cover the total length of the air distribution pipe. The total mass flow of air was kept constant for all simulations. The air outlet velocity was thus lower than for the initial design. The simulations were repeated where the secondary air row was tilted in steps of 12° until vertical position.

Results from all six simulations showed that the gas flow through the side face mixes well but in all cases the front face indicates a high temperature. The contour plots for all cases indicated similar shapes. Therefore tilting of the secondary air row does not affect the results in any major way. The only discrepancy seen is that the mass flow through the front face decreases when the secondary air row is tilted vertically upwards.

Simulations where the secondary air row was further tilted, *i. e.* the holes were facing outside the roof, led to unsatisfactory mixing of the gas flow along the side of the distribution pipe.

To improve the mixing (lower the temperature) on the front face, secondary air was introduced close to this face. Several simulations were performed with different numbers, sizes and positions of holes. The results showed that all three variables are of utmost importance. Still some areas had too high a temperature (poor mixing) on the front and side faces. The air velocity through the holes was too low to penetrate the gas flow leaving the burner. Since the total mass flow was constant, the simulations revealed that relocation of the air distribution was necessary in order to improve the mixing.

For primary air the number of holes and their sizes were decreased in order to increase the velocity through the remaining holes. The holes at the end of the distribution pipe were resized, the position was changed and some of the holes were deleted. Finally the secondary air row was changed to 26 holes with the same diameter and a uniform distance between the holes. These changes increased the velocity to 23 m/s. With the secondary air row in vertical position, 20.7% of the total mass flow passed through the front face. Good mixing on the front face is presented in fig. 8 (left), while the side face now needed some improvement.

Earlier simulations demonstrated small changes in mixing rate for different elevations of the secondary air row. The main difference was an increased flow through the front face when changing from vertical position. To increase the residence time for the mixture of flue gas and

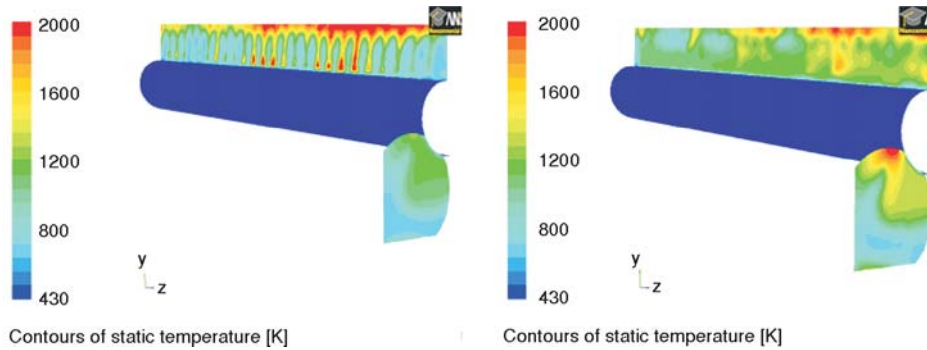


Figure 8. Contour plot of temperature distribution on side and front faces. Vertical secondary air (left) and 24° tilted (right)

secondary air in a hot environment, the secondary air row was tilted 24° from the vertical line. The temperature profile (fig. 8, right)) for the side face was improved compared to fig. 8 (left) as a result of tilting the secondary row, but the front face had the opposite development. The gas flow through this face had increased. 26.4% of the total mass flow was then passing through the front face and causing the locally increased temperature (*i. e.* poor mixing).

A vector plot of velocity showed that hot gases from the fuel bed rise upwards towards the roof and forwards. At the end of the burner there is a wall and the gas flow is forced downwards along this wall and leaves the burner through the top of the front face. This flow causes the hot region in fig. 8 (right). It needs to be eliminated with secondary air. The holes were therefore changed.

The small face between the roof and the vertical wall was closed. The velocity was set at 20.7 m/s to ensure a total mass flow according to the pre-determined value. The mass flow through the front face changed to 26%. Figure 9 still points out some high temperature regions. On the side face, these regions are located near secondary air holes of smaller size.

After this parametric study, the axial distribution of air supply resulting from the air pipe simulations was introduced. The velocity was given a value according to the holes' positions along the air distribution pipe. The lowest velocity was set close to the fuel inlet and the highest values at the opposite end; see fig. 4. The difference in velocity between the first and the last hole was set at 30%. The primary air row 1 consisted of 11 holes and the last hole (seen from fuel inlet) had an increased diameter compared to the other 10. The primary air row 2 consisted of 10 holes with the same diameter; the last two holes in the row had an increased diameter.

The secondary air row (24° from the vertical line) had 26 holes. Two different diameters were used depending on the hole location. Close to the front face, one hole was set between the primary air rows 1 and 2. Another two holes were located 50° from the vertical line in the

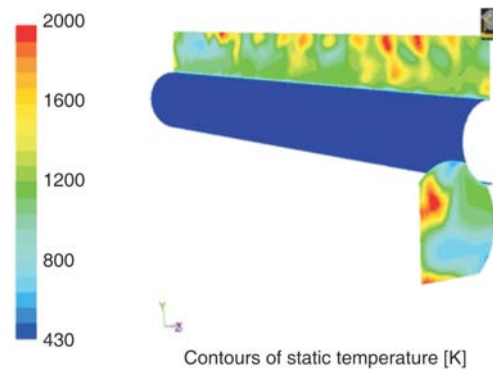


Figure 9. Contour plot of temperature distribution on side and front faces, relocation of the holes at the end of the pipe

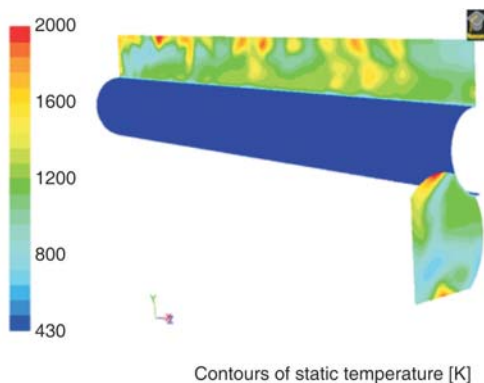


Figure 10. Contour plot of temperature distribution on side and front faces, optimised design

ter release from the holes of the secondary air row to the actual position. The time available for reaction between the flue gas and the secondary air after they are reasonably well mixed and until the temperature is too low for effective oxidation of CO to take place, can be estimated with fig. 11. This gives a residence time in the hot environment (down to orange in fig. 11 (left)) that is shorter than 0.01 s.

same zone. Finally, a hole was placed 66° from the vertical line with a smaller diameter compared to the other holes in this zone and closer to the vertical wall in order to improve the mixing close to the top of the front face. With this configuration all regions with maximum temperature vanished and an optimised solution was obtained, fig. 10. The flow through the front face was 25.3% of total air mass flow. 1% of the total mass flow passed from the burner through the end part of the fuel bed. The rest of the flow passed through the side face.

Figure 11 (left) shows the temperature in the furnace at a plane 105 mm from the fuel inlet. Figure 11 (right) shows path lines for secondary air, the colours indicating the time for the air after

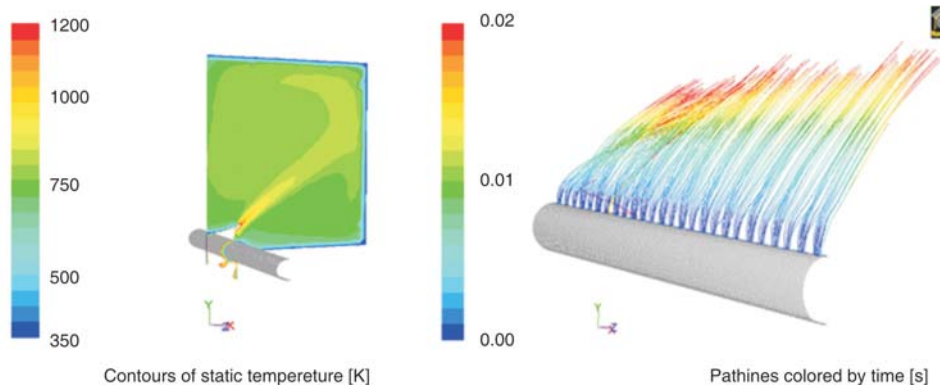


Figure 11. (Left) contour plot of temperature distribution on a face 105 mm from fuel inlet, (right) path lines for secondary air

Validation

The optimisation performed with CFD resulted in a new design of air supply according to the final results from the sub-section *Burner optimisation*. New air distribution pipes were installed. The burner was fired with wood pellet, which gave a power output of 19.2 kW.

Figure 12 shows that the combustion on the bed starts close to the fuel inlet indicating a larger active fuel bed than before, which allows the desired power output. The secondary air is directed under the roof of the burner, so the flue gas is mixed with secondary air in a hot environment. However, the residence time in this hot environment is still very short, which may explain

why there are still levels of emissions of carbon monoxide that may be reduced in a secondary combustion zone.

The excess air was reduced without increasing the emissions of CO compared to the initial design. The average emission of oxygen during this experiment was 7.5% with 316 ppm of CO normalised to 10% O₂.

The effect of residence time in a secondary zone might have been captured by including combustion in the simulation, requiring the use of kinetic models. Kinetic models for combustion are unfortunately not reliable. Furthermore, they make numerical convergence more difficult and require additional computational capacity.



Figure 12. Combustion with optimised air supply

Estimation of residence time

The necessary residence time to burn CO in the secondary zone can be estimated with the eq. (1) in Haywood [14]:

$$\frac{d[\text{CO}]}{dt} = -4.3 \cdot 10^{11} \cdot [\text{CO}][\text{O}_2]^{0.25} \exp\left(-\frac{E}{RT}\right) \quad (1)$$

where $[\]$ denotes the concentration in gram moles per cm³ and $E/R = 20000$ K

Assuming a reasonable composition of the combustible gases from the bed and temperature of the mixture of air and these gases of 1000 K, the time needed for combustion is calculated at 0.07 s with the above model.

At a higher temperature, say 1273 K, the corresponding time would decrease to about 0.0013 s.

The simulation gave a residence time below 0.01 s while the mixing temperature was high enough. This short residence time may explain the relatively high values of CO emissions in the experiments with the final design of the air supply. In summary the burner does not have a big enough secondary combustion zone for satisfactory combustion.

The analytical calculations require perfectly mixed gases. The estimated time is therefore considerably underestimated and should be compared with an often used rule of thumb of 2 s in a hot environment. This includes time for mixing and reaction to take place. With forced mixing the time needed is well below 2 s.

Conclusions

A numerical methodology to optimise a combustion unit has been developed and validated with a concrete test case. The numerical optimisation aims to increase the mixing of species. The method uses CFD, where chemical reactions have been omitted. The model involves the mixing of only one species, air, where the Navier-Stokes equations are solved together with the energy equation. The amount of fuel needed for a power output is easy to establish and the amount of air needed is theoretically calculated or determined with some combustion software.

The relation between primary and secondary air can be chosen from experience when the fuel and its moisture content are known.

Application of the methodology to a pellets burner enabled successful emplacement of the primary and secondary air feeding holes. Experiments show an increase of the power output from 15 to 19.2 kW and a considerable decrease of CO. The combustion unit may be further improved by the addition of a secondary combustion chamber increasing the residence time.

Acknowledgments

This work has been carried out thanks to funding from the Swedish National Energy Administration (STEM), Swebo Bioenergy and the County Administrative Board of Norrbotten.

References

- [1] Hirmsmark, J., *Densified Biomass Fuels in Sweden-Country Report for the EU/INDEF Project*, Department of Forest Management and Products, Swedish University of Agriculture Science, Uppsala, Sweden, 2002
- [2] Mani, S., *et al.*, *Economics of Producing Fuel Pellets from Biomass*, American Society of Agriculture and Biological Engineers, St. Joseph, Mich., USA, 2006
- [3] Hoglund, J., *The Swedish Fuel Pellets Industry, Production, Market and Standardization*, Department of Forest Management and Products, Swedish University of Agriculture Science, Uppsala, Sweden, 2008
- [4] Ronnbock, M., Johansson, M., Claesson, F., *ERA-Net Evaluation of Development Status of Small-Scale Combustion Units Using Pellets from New Materials with a High Content of Ash*, SP-rapport 2008:31, SP-Technical Research Institute of Sweden, Boras, Sweden, 2008
- [5] Porso, C., *The Effect of New Raw Materials on Pellets Prices*, Examensarbete 2010:01, SLU, Swedish University of Agriculture Science, Uppsala, Sweden, 2010
- [6] Jordan, C., Harasek, M. *Improvement of a Combustion Unit Based on a Grate Furnace for Granular Dry Solid Biofuels Using CFD Methods*, *Heat Transfer Engineering*, 31 (2010), 9, pp. 774-781
- [7] Porteiro, J., *Numerical Modeling of a Biomass Pellet Domestic Boiler*, *Energy & Fuels*, 23 (2009), 2, pp. 1067-1075
- [8] Wang, Y., Yan, L., *CFD Studies on Biomass Thermochemical Conversion*, *Int. J. Mol. Sci.*, 9 (2008), 9, pp. 1108-1130
- [9] Klason, T., Bai, X. S., *Computational Study of the Combustion Process and NO Formation in a Small-Scale Wood Pellet Furnace*, *Fuel*, 86 (2007), 10-11, pp. 1465-1474
- [10] Norin, B., *STEM Rapport 21310 – Etapp 2; Burners for Fuels with a High Content of Ash*
- [11] ***, *FlueGas*, Commercial Software Sold by MM EnviLoop AB
- [12] Cengel, Y. A., Turner, R. H., *Fundamentals of Thermal-Fluid Sciences*, McGraw-Hill, New York, USA, 2001
- [13] ***, *ANSYS FLUENT (2009), Ansys Fluent 12.0 user guide*, ANSYS Inc.
- [14] Haywood, J. B., *Internal Combustion Engine Fundamentals*, McGraw-Hill, New York, USA, ISBN 0-07-028637-X